AIP | Journal of Applied Physics

Tailoring of unipolar strain in lead-free piezoelectrics using the ceramic/ceramic composite approach

Neamul H. Khansur, Claudia Groh, Wook Jo, Christina Reinhard, Justin A. Kimpton, Kyle G. Webber, and John E. Daniels

Citation: Journal of Applied Physics **115**, 124108 (2014); doi: 10.1063/1.4869786
View online: http://dx.doi.org/10.1063/1.4869786
View Table of Contents: http://scitation.aip.org/content/aip/journal/jap/115/12?ver=pdfcov
Published by the AIP Publishing

Tailoring of unipolar strain in lead-free piezoelectrics using the ceramic/ceramic composite approach

Neamul H. Khansur,[1] Claudia Groh,[2] Wook Jo,[2] Christina Reinhard,[3] Justin A. Kimpton,[4] Kyle G. Webber,[2] and John E. Daniels[1]
[1]*School of Materials Science and Engineering, University of New South Wales, NSW 2052, Australia*
[2]*Institute of Materials Science, Technische Universität Darmstadt, Alarich-Weiss-Straße 2, 64287 Darmstadt, Germany*
[3]*Diamond Light Source, Beamline I12 JEEP, Didcot, Oxfordshire OX11 0DE, United Kingdom*
[4]*The Australian Synchrotron, Clayton, Victoria 3168, Australia*

(Received 23 February 2014; accepted 17 March 2014; published online 27 March 2014)

The electric-field-induced strain response mechanism in a polycrystalline ceramic/ceramic composite of relaxor and ferroelectric materials has been studied using *in situ* high-energy x-ray diffraction. The addition of ferroelectric phase material in the relaxor matrix has produced a system where a small volume fraction behaves independently of the bulk under an applied electric field. Inter- and intra-grain models of the strain mechanism in the composite material consistent with the diffraction data have been proposed. The results show that such ceramic/ceramic composite microstructure has the potential for tailoring properties of future piezoelectric materials over a wider range than is possible in uniform compositions. © *2014 AIP Publishing LLC*.
[http://dx.doi.org/10.1063/1.4869786]

INTRODUCTION

Piezoelectric materials are used in a wide range of industrial and consumer applications with the market largely dominated by the lead-based composition $Pb(Zr,Ti)O_3$ (PZT).[1] Considering PZT's environmental concerns and limitations in high temperature performance, research into lead-free electroceramics has increased dramatically in the last decade.[2] New synthesis routes and information gained from detailed structural studies of existing high-performance lead-free compositions are leading to the development of new compositions of interest. From extensive knowledge of the PZT system, a common approach for the development of lead-free compositions is to search for systems with morphotropic phase boundary (MPB). Promising lead-free ferroelectrics (FEs) include compositions based on sodium potassium niobate $Na_{(1-x)}K_xNbO_3$ (KNN) and bismuth sodium titanate $Bi_{1/2}Na_{1/2}TiO_3$ (BNT).[3–8] In 2007, Zhang *et al.*[9] reported a new pseudo-ternary composition, replacing a small fraction of BNT with KNN from the $Bi_{1/2}Na_{1/2}TiO_3$-$BaTiO_3$ (BNT-BT) system, which showed large electric-field-induced strain values (0.45% at 8 kV/mm). This field-induced strain response remains stable against temperature[10] and cyclic fatigue.[11] While the strain response of this material is attractive for actuator applications, it is limited in device implementation due to the high actuating field ($\geq$6 kV/mm) and significant hysteresis. Several other BNT-based compositions with large strain have been reported by different authors.[12–14] Interestingly, among all these compositions the strain is generated via an electric-field-induced reversible transition between pseudocubic relaxor (RE) and non-cubic ferroelectric phases at relatively high fields ($\geq$4 kV/mm).[15–18] Further improvement of actuator properties with such compositions will require the lowering of the actuating field. One possible approach for achieving this is to modify the microstructure of these materials using a ceramic/ceramic composite method.

Producing ceramic/ceramic composites with a controlled microstructure in order to tailor the electrical properties (such as dielectric, piezoelectric, and pyroelectric) in electroceramics is a well-known approach.[19–21] However, it has not been applied to modify the properties of large strain BNT-based lead-free materials until recently. Several studies[22–27] have introduced ceramic/ceramic composite systems as a method to tune the electrical and electro-mechanical properties in lead-free ferroelectrics. Lee *et al.*[22] have focused on the minimization of the actuating field of large strain BNT materials by forming a compositionally non-homogeneous phase structure (relaxor and ferroelectric) at the grain length scale. They showed that the actuating field can be significantly reduced with the addition of 20 vol. % of ferroelectric grains in the matrix of relaxor grains. The improved properties of the ceramic/ceramic composite material have been explained by a series capacitor model where polarisation coupling throughout the material reduces the required actuating fields.[22,26] Wada *et al.*[23,25] have reported another type of compositionally non-homogeneous barium titanate-potassium niobate $BaTiO_3$-$KNbO_3$ (BT-KN) ceramic. In this system, an artificial MPB has been created between single crystal particles of BT and an epitaxial shell of KN. Strain response in this very same composition was reported by Fujii *et al.*[24] and it has been found that the BT-KN composite exhibit approximately three times larger strain than the BT-KN solid solution ceramics.[28] This comparatively large strain response in BT-KN composite has been attributed to the polarization rotation at the strained epitaxial interface region.[24] These studies show the ceramic/ceramic composite structure is a promising path for the development of future lead-free electro-mechanical materials.

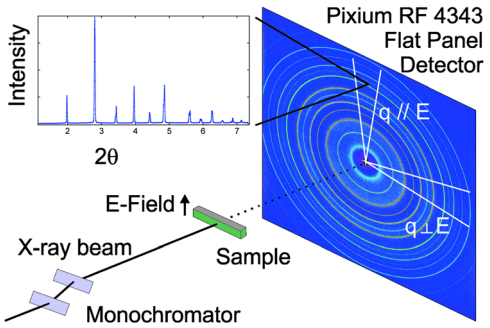

FIG. 1. Schematic of experimental geometry and collected diffraction pattern with large area 2D detector. Inset shows a typical diffraction pattern from the area detector after radial integration.

The development of new lead-free ceramic/ceramic composites for industrial applications will benefit from a detailed understanding of the underlying strain generation mechanisms. An attempt has been made in this paper to highlight the strain generation mechanism in recently reported 0.92BNT-0.06BT-0.02KNN (BNT-BT-2KNN) and 0.93BNT-0.07BT (BNT-7BT) ceramic/ceramic composite materials[26,27] using *in situ* high-energy x-ray diffraction. The large strain BNT-BT-2KNN composition shows a reversible transition between a relaxor and ferroelectric phase with applied external electric field, while BNT-7BT shows an irreversible phase transition to the ferroelectric state.[29] In these ceramic/ceramic composite systems, the effect of volume fraction of FE phase BNT-7BT on the reversible transition of the relaxor (RE) phase BNT-BT-2KNN has been studied *in situ* using high-energy x-ray diffraction.[15,18] The macroscopically measured strain response has been correlated with the structural response. A microscopic strain mechanism has been proposed on the basis of diffraction studies.

EXPERIMENTAL

The ceramic/ceramic composite materials were prepared using FE $0.93(Bi_{1/2}Na_{1/2}TiO_3)$-$0.07(BaTiO_3)$ (BNT-7BT) as a particulate component and RE $0.92(Bi_{1/2}Na_{1/2}TiO_3)$-$0.06(BaTiO_3)$-$0.02(K_{1/2}Na_{1/2}NbO_3)$ (BNT-BT-2KNN) as the matrix component. Six different compositions have been prepared by varying the volume fraction of FE (0FE, 10FE, 20FE, 30FE, 50FE, and 100FE). Details of the synthesis route have been previously reported.[26,27] Macroscopic unipolar strains up to fields of 6 kV/mm were measured with disk-shaped samples by modified sawyer tower setup at a frequency of 50 mHz. Bar-shaped ceramic samples of 0.8 mm × 1 mm × 6 mm suitable for *in situ* high-energy diffraction experiments were cut from sintered disks. Silver electrodes were applied to two opposing 1 mm × 6 mm faces of the bar.

In situ high-energy x-ray diffraction measurements were carried out at beamline I12-JEEP of the Diamond Light Source, UK. A monochromatic x-ray beam of energy 84.82 keV (wavelength $\lambda = 0.146$ Å) and dimensions 150 μm × 150 μm was used. Diffraction patterns were collected in transmission geometry using a large area detector as shown schematically in Figure 1. The detector parameters, including distance, beam centre, and tilts, were calibrated using a standard ceria powder pattern. For the diffraction patterns to be measured *in situ*, samples were placed in a specifically designed electric field chamber where the applied electric field is perpendicular to the x-ray beam direction.[30] In this geometry, diffraction information is simultaneously collected with the scattering vector at all possible angles to the applied field vector.

Diffraction images were collected during an applied unipolar electric field up to 6 kV/mm in steps of 0.6 kV/mm. These images were integrated into 36 azimuthal sections with 10° intervals using the software package FIT2D.[31] Single or multiple pseudo-Voigt fitting functions have been fit to selected peaks within the diffraction patterns. The refined peak positions have been used in the following equation to calculate the lattice strain as a function of applied electric field

$$\varepsilon_{hkl} = -\Delta\theta \cot\theta_0$$

where ε_{hkl} is the lattice strain for specific *hkl* plane, θ_0 is the diffracted angle of the *hkl* reflection at initial state, and $\Delta\theta$ is the difference between the diffraction angle of the strained state and initial state.

RESULTS AND DISCUSSIONS

The microstructure of the samples used in the current study has been investigated by SEM, TEM, and and energy-dispersive x-ray (EDX).[26,27] It is found that the average grain size of the samples is approximately 2 μm and is consistent over the compositional range reported here. Compositionally sensitive measurements were performed on the 10FE and 50FE compositions and showed that the materials have sub-grain regions approximately 0.05 μm in size that are niobium rich. Additionally, grains containing these Nb rich areas were also sodium (Na) and potassium (K) rich. These previous results confirm that compositional inhomogeneity exists in such materials.

Macroscopically measured unipolar strain at 6 kV/mm for different ceramic/ceramic composite is shown in Figure 2(a). Characteristic parameters were derived from these strain loops as presented in Figure 2(b) showed interesting trends in electrical properties as a function of particulate FE phase. The poling strain value at maximum field (6 kV/mm) varies from 0.39 to 0.45% and is maximum for pure FE (100FE) materials. E_{pol} represents the field strength at which the sample is poled from the as-processed state; E_{pol} tends to decrease with increasing amount of FE phase. The effect of volume fraction of FE phase is more pronounced in the remnant strain which increases from zero for the pure relaxor (RE) phase material to 0.26% for the pure FE phase material.

With 0%FE, no remnant strain is observed in the material due to a reversible structural transformation[9,15] with applied field, which is characteristic of this composition. With increasing amount of FE phase the ceramic/ceramic composite materials shows an increasing remnant strain that is maximum for pure FE materials (100FE). The remnant strain for 100FE is consistent with previous measurements reported for BNT-7BT that show a remnant strain of 0.24% (Ref. 32) resulting from an irreversible phase

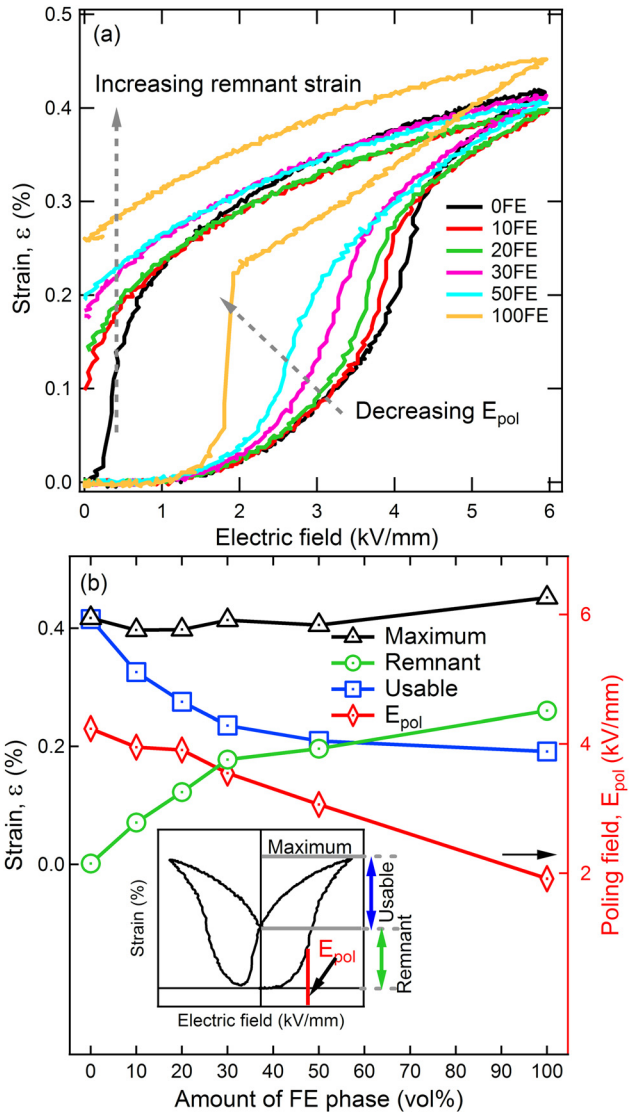

FIG. 2. (a) Unipolar strain hysteresis and (b) derived characteristic parameters of macroscopic strain (schematic illustration of derived characteristic parameters is shown in the inset) for ceramic/ceramic composite at 6 kV/mm. With increasing FE content the remnant strain increases, while the poling strain at maximum field is approximately constant. The usable strain reduces with increasing FE content.

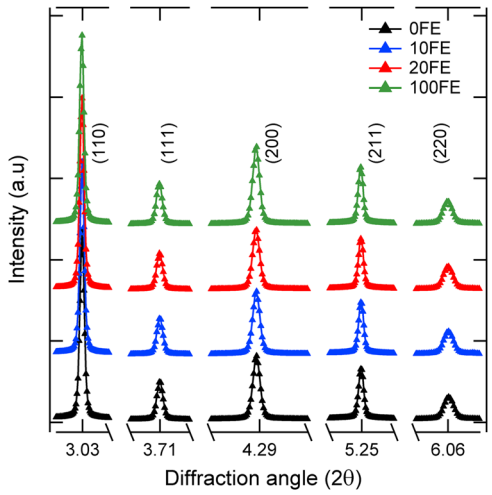

FIG. 3. Experimental diffraction profiles for four different compositions in the as-processed state. Single and symmetric diffraction peaks are seen throughout the patterns indicating a pseudocubic structure.

transformation.[18] In this case, with a maximum applied field of 6 kV/mm, the usable strain (i.e., maximum strain – remnant strain) decreases continuously with increasing fraction of FE phase.

In situ high-energy x-ray diffraction experiments have been carried out for all the compositions. Four selected compositions (0FE, 10FE, 20FE, and 100FE) have been presented here to elucidate the strain mechanism in relaxor/ferroelectric composites. All of the compositions in the as processed state show single phase perovskite type diffraction patterns that can be indexed with a cubic $Pm\bar{3}m$ structure (Figure 3). The samples show electrical properties not consistent with pure cubic phase materials. Additionally, it is known that small distortions at the local scale exist in related compounds;[33,34] therefore, the structure of the as-processed material is referred to as pseudocubic. No significant difference in the lattice parameter is observed for the four compositions within the resolution of the diffraction instrument used. However, the macroscopic strain response behaviour is significantly different for each composition; thus, it can be assumed that these crystallographically similar compositions are responding differently under applied electric fields.

The electric-field-induced transformation behaviour in such perovskite materials can be qualitatively characterized by observing the (111) and (200) type pseudocubic reflections. *In situ* diffraction patterns for (111) and (200) type pseudocubic peaks of all four compositions with the electric field vector aligned with the diffraction scattering vector are presented in Figure 4. The 0FE composition (Figure 4(a)) shows a maximum lattice strain of 0.06% and 0.15% at 6 kV/mm (E_{max}) in the (111) and (200) peaks, respectively. No shoulder peak is observed in the (200) peak as shown in the bottom of Figure 4(a). This observed lattice strain is completely reversible, and the peaks return to their original positions upon removal of the electric field. This reversible electric-field-induced lattice strain behaviour is characteristic of relaxor type high-strain materials.[15]

Data presented in Figure 4(b) for the 100FE composition show that the application of electric field of 6 kV/mm (E_{max}) induces significant distortions in the (111) and (200) peaks. These distortions remain after the electric field is removed (E_{rem}). Thus, it can be said that this composition shows an irreversible electric-field-induced phase transformation. The nature of phase transformation in this system has been previously reported as either pseudocubic to tetragonal or pseudocubic to mixed phase tetragonal and rhombohedral.[18,35] The observed (111) peak distortion and (002)/(200) peak splitting reveals that the field-induced transformation for the composition in this study is likely a mixed phase type transformation.

Figure 4(c) shows the 10FE composition (111) and (200) diffraction patterns under the applied electric field. A lattice strain of 0.07% and 0.18% is observed at 6 kV/mm in the (111) and (200) peaks, respectively. The (200) peak in this composition develops a small low 2θ shoulder under the applied field. It also exhibits remnance in lattice strain after

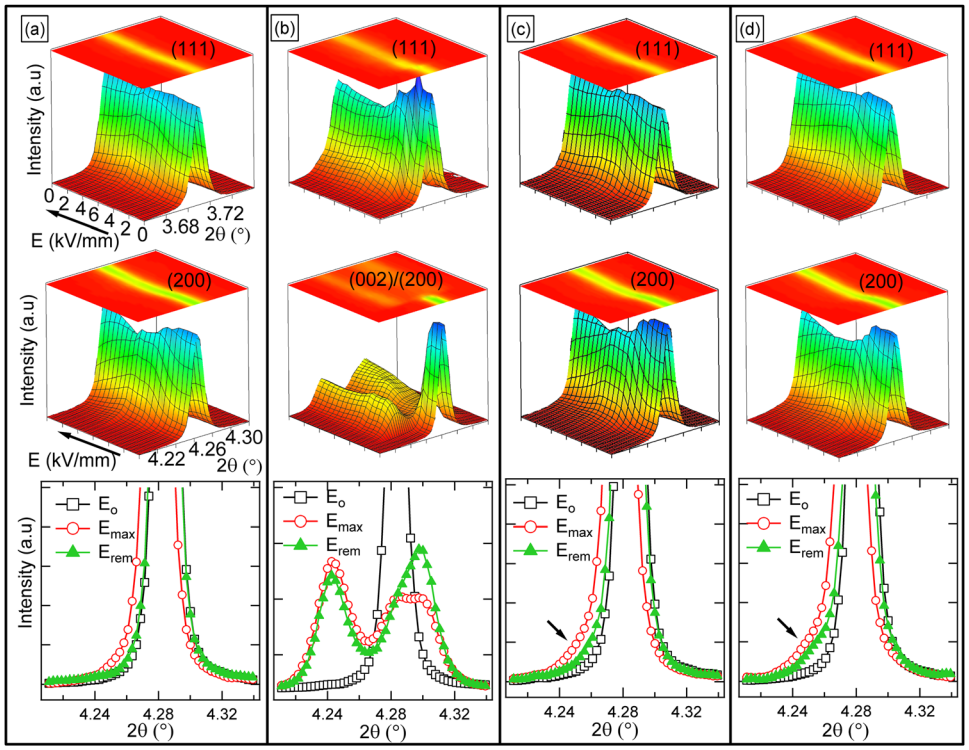

FIG. 4. (111) (top) and (200) (middle) diffraction peaks for (a) 0%FE, (b) 100%FE, (c) 10%FE, and (d) 20%FE materials as function of applied electric field. The variation in (200) shoulder peak intensity in as-prepared (E_0), at 6 kV/mm (E_{max}) field and after removal of electric field (E_{rem}) for all compositions (bottom). These data represent scattering information with the applied electric field vector parallel to the diffraction scattering vector.

the removal of electric field (correlating with the macroscopic strain, Figure 2).

Figure 4(d) represents (111) and (200) diffraction patterns for the 20FE composition under the applied electric field. A lattice strain of 0.08% and 0.18% is observed at 6 kV/mm in the (111) and (200) peaks, respectively. The (200) peak in this composition, however, reveals more information about the generated strain. Inset of Figure 4(d) shows the low 2θ shoulder of the (200) diffraction peak develop during the application of the electric field in 20FE ceramic/ceramic composite. The shoulder of (200) peak is more pronounce in 20FE (bottom of Figure 4(d)) composition than the 10 FE (bottom of Figure 4(c)). Thus, it can be assumed that development of the low 2θ shoulder depends on increasing volume fraction of FE phase in the ceramic/ceramic composite. The development of the shoulder during the application of the electric field is consistent with a small volume fraction of the bulk material undergoing a pseudocubic to tetragonal phase transformation. In the ceramic/ceramic composite studied here, this would imply that the small volume fraction of particulate phase has undergone the irreversible transition to the ferroelectric state, while the bulk of the sample has reversible electric-field-induced strain consistent with a conventional relaxor material. In other words, compositions, such as 10FE and 20FE, exhibit a combined effect of 0FE and 100FE in their field-induced response; as evident from the diffraction data.

Based on the *in situ* diffraction results, microscopic strain response mechanisms for ceramic/ceramic composite have been proposed (Figure 5). At the initial zero field state, the ceramic/ceramic composite can be represented as a polycrystalline ceramic composed of relaxor (RE) grains (Figure 5(a)). With the application of electric field differences in field-induced transformation in ceramic/ceramic composite can be visualized either by Figure 5(b) (type I) or Figure 5(d) (type II), where former shows inter-grain and latter shows intra-grain composite effects. In the proposed type I mechanism, ferroelectrically/ferroelastically strained FE grain induces a ferroelectric state on the neighbouring RE grains. This similar kind of induced effect can occur in smaller regions as shown in type II. With further increase in electric field (Figures 5(c) and 5(e)) the switched ferroelectric domains propagate strain on the surrounding RE matrix. A majority fraction of the strained region can be relaxed back with the removal of electric field but not completely.

The proposed model based on the *in situ* diffraction study suggests that the addition of FE phase materials at later stages of processing has produced a polycrystalline material where regions at the grain scale behave independently of the bulk. This has significant implications for the response mechanism of such materials. In particular, the length scale and magnitude of the compositional inhomogeneity may be tuned to increase local responses that may propagate throughout the material. Bintachitt *et al.*[36] has reported that in PZT thin films, nonlinear response of piezoelectricity is not homogeneous throughout a compositionally uniform sample, i.e., piezoelectric nonlinear response shows local deviation from the average due to difference in domain wall pinning. A local deviation in electric field distribution, polarisation, and strain response has been shown by Jayabal *et al.*[37,38] for bulk materials by micromechanical modelling. This local deviation has been attributed to the domain

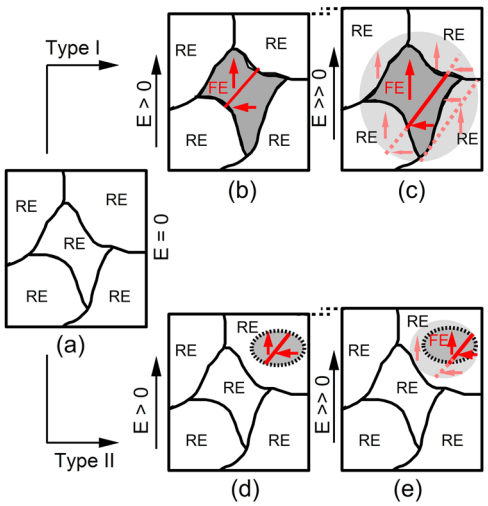

FIG. 5. Representation of proposed mechanisms of electric-field-induced strain generation. (a) Ceramic/ceramic composite in as-processed state without any FE domains; for simplicity, all the grains have been labelled as RE. Depending on the spatial distribution of compositional inhomogeneity when the field is applied it can follow either of the type I ((b) and (c)) or type II ((d) and (e)) mechanism. Type I showing the inter-grain composite effect where one of the grain irreversibly transforms from RE to FE (b) and with further increase in electric field the FE domains propagate to the surrounding RE grains (c). Type II shows the intra-grain composite effect where a region of RE grain irreversibly transforms into FE phase (d). Reversible transformation of RE phase has not been shown here for clarity.

switching processes at the individual grain length scale. As the individual grains in polycrystalline ceramics do not behave uniformly under an applied field; tuning the microstructure by incorporating different phase grains can adjust the macroscopic properties. Here, we have shown that the electric-field induced strain response of BNT-7BT grains in a polycrystalline ceramic/ceramic composite is dictating (or coupled with) the strain response behaviour of the relaxor matrix. Thus, the local response of the particulate phase can be used to tune or nucleate specific behaviour to the bulk materials properties. The potential for tailoring the properties of functional ceramics using ceramic/ceramic composite structures at the granular scale therefore exists.

CONCLUSIONS

The electric-field-induced strain response in a ceramic/ceramic composite of relaxor and ferroelectric materials has been investigated by means of *in situ* high-energy x-ray diffraction. Evaluated microscopic strain response behaviour from diffraction information has been correlated with the macroscopic strain response for two ceramic/ceramic compositions (10FE and 20FE) and the two constituents (0FE and 100FE). It has been found that in the as-processed state 10FE and 20FE exhibit a pseudocubic structure similar to 0FE and 100FE. With applied electric field cycle 0FE showed reversible lattice strain, whereas 100FE showed an irreversible phase transformation. In the 10FE and 20FE composition data are consistent with a model where regions of FE grains transformed independent of the bulk. Based on the diffraction study models for microscopic strain generation in ceramic/ceramic composites have been proposed.

ACKNOWLEDGMENTS

This work was supported in part by ARC Discovery Grant No. DP120103968 and Deutsche Forschungsgemeinschaft (DFG) under SFB595. J.E.D. acknowledges the financial support through an Australian Institute of Nuclear Science and Engineering Research Fellowship. C.G. and W.J. acknowledge the financial support from the state centre AdDIA on adaptronics. Part of the travel funding (J.A.K.) was supported by the International Synchrotron Access Program (AS/IA123/5658). K.G.W. gratefully acknowledges the support of the Deutsche Forschungsgemeinschaft under WE4972/2-1. This work was carried out with the support of the Diamond Light Source under the experiment No. EE8019.

[1]N. Setter, J. Eur. Ceram. Soc. **21**, 1279 (2001).
[2]J. Rödel, W. Jo, K. T. P. Seifert, E. M. Anton, T. Granzow, and D. Damjanovic, J. Am. Ceram. Soc. **92**(6), 1153 (2009).
[3]L. Egerton and D. M. Dillon, J. Am. Ceram. Soc. **42**(9), 438 (1959).
[4]G. A. Smolensikii, V. A. Isupov, A. I. Agranovskaya, and N. N. Krainik, Sov. Phys. Solid State **2**, 2651 (1961).
[5]T. Takenaka, K. I. Maruyama, and K. Sakata, Jpn. J. Appl. Phys., Part 1 **30**(9B), 2236 (1991).
[6]K. Sakata and Y. Masuda, Ferroelectrics **7**(1), 347 (1974).
[7]Y. Hiruma, H. Nagata, and T. Takenaka, J. Appl. Phys. **104**(12), 124106 (2008).
[8]Y. Makiuchi, R. Aoyagi, Y. Hiruma, H. Nagata, and T. Takenaka, Jpn. J. Appl. Phys., Part 1 **44**(6B), 4350 (2005).
[9]S. T. Zhang, A. B. Kounga, E. Aulbach, H. Ehrenberg, and J. Rodel, Appl. Phys. Lett. **91**, 112906 (2007).
[10]S. T. Zhang, A. B. Kounga, E. Aulbach, W. Jo, T. Granzow, H. Ehrenberg, and J. Rodel, J. Appl. Phys. **103**(3), 034108 (2008).
[11]Z. Luo, T. Granzow, J. Glaum, W. Jo, J. Rödel, and M. Hoffman, J. Am. Ceram. Soc. **94**(11), 3927 (2011).
[12]E. M. Anton, W. Jo, J. Trodahl, D. Damjanovic, and J. Rödel, Jpn. J. Appl. Phys. **50**, 055802 (2011).
[13]V.-Q. Nguyen, H.-S. Han, K.-J. Kim, D.-D. Dang, K.-K. Ahn, and J.-S. Lee, J. Alloys Compd. **511**(1), 237 (2012).
[14]K.-N. Pham, A. Hussain, C. W. Ahn, W. Kim Ill, S. J. Jeong, and J.-S. Lee, Mater. Lett. **64**(20), 2219 (2010).
[15]J. E. Daniels, W. Jo, J. Rödel, V. Honkimäki, and J. L. Jones, Acta Mater. **58**(6), 2103 (2010).
[16]A. J. Royles, A. J. Bell, A. P. Jephcoat, A. K. Kleppe, S. J. Milne, and T. P. Comyn, Appl. Phys. Lett. **97**(13), 132909 (2010).
[17]J. Hao, B. Shen, J. Zhai, C. Liu, X. Li, and X. Gao, J. Appl. Phys. **113**(11), 114106 (2013).
[18]J. E. Daniels, W. Jo, J. Rödel, and J. L. Jones, Appl. Phys. Lett. **95**(3), 032904 (2009).
[19]O. Furukawa, M. Harata, M. Imai, Y. Yamashita, and S. Mukaeda, J. Mater. Sci. **26**(21), 5838–5842 (1991).
[20]H. Komiya, Y. Naito, T. Takenaka, and K. Sakata, Jpn. J. Appl. Phys., Part 1 **28S2**(Supplement 28–2), 114 (1989).
[21]A. Yoneda, T. Takenaka, and K. Sakata, Jpn. J. Appl. Phys., Part 1 **28S2**(Supplement 28–2), 95 (1989).
[22]D. S. Lee, D. H. Lim, M. S. Kim, K. H. Kim, and S. J. Jeong, Appl. Phys. Lett. **99**(6), 062906 (2011).
[23]S. Wada, S. Shimizu, K. Yamashita, I. Fujii, K. Nakashima, N. Kumada, Y. Kuroiwa, Y. Fujikawa, D. Tanaka, and M. Furukawa, Jpn. J. Appl. Phys., Part 1 **50**(9), 09NC08 (2011).
[24]I. Fujii, S. Shimizu, K. Yamashita, K. Nakashima, N. Kumada, C. Moriyoshi, Y. Kuroiwa, Y. Fujikawa, D. Tanaka, M. Furukawa, and S. Wada, Appl. Phys. Lett. **99**(20), 202902 (2011).
[25]S. Wada, K. Yamashita, I. Fujii, K. Nakashima, N. Kumada, C. Moriyoshi, Y. Kuroiwa, Y. Fujikawa, D. Tanaka, and M. Furukawa, Jpn. J. Appl. Phys., Part 2 **51**(9), 09LC05 (2012).
[26]C. Groh, D. J. Franzbach, W. Jo, K. G. Webber, J. Kling, L. A. Schmitt, H.-J. Kleebe, S.-J. Jeong, J.-S. Lee, and J. Rödel, Adv. Funct. Mater. **24**(3), 356 (2014).

[27]C. Groh, W. Jo, and J. Rödel, "Tailoring Strain Properties of $(0.94-x)Bi_{1/2}Na_{1/2}TiO_3-0.06BaTiO_3-xK_{0.5}Na_{0.5}NbO_3$ Ferroelectric/Relaxor Composites," J. Am. Ceram. Soc. (published online).
[28]S. Wada, M. Nitta, N. Kumada, D. Tanaka, M. Furukawa, S. Ohno, C. Moriyoshi, and Y. Kuroiwa, Jpn. J. Appl. Phys., Part 1 **47**(9), 7678 (2008).
[29]W. Jo, R. Dittmer, M. Acosta, J. Zang, C. Groh, E. Sapper, K. Wang, and J. Rödel, J. Electroceram. **29**, 71 (2012).
[30]J. Daniels, A. Pramanick, and J. Jones, IEEE Trans. Ultrason. Ferroelectr. Freq. Control **56**(8), 1539 (2009).
[31]A. P. Hammersley, S. O. Svensson, M. Hanfland, A. N. Fitch, and D. Hausermann, High Pressure Res. **14**, 235 (1996).
[32]W. Jo and J. Rodel, Appl. Phys. Lett. **99**, 042901 (2011).
[33]J. Kreisel, P. Bouvier, B. Dkhil, P. Thomas, A. Glazer, T. Welberry, B. Chaabane, and M. Mezouar, Phys. Rev. B **68**(1), 014113 (2003).
[34]J. E. Daniels, W. Jo, J. Rodel, D. Rytz, and W. Donner, Appl. Phys. Lett. **98**(25), 252904 (2011).
[35]H. Simons, J. Daniels, W. Jo, R. Dittmer, A. Studer, M. Avdeev, J. Rodel, and M. Hoffman, Appl. Phys. Lett. **98**(8), 082901 (2011).
[36]P. Bintachitt, S. Jesse, D. Damjanovic, Y. Han, I. Reaney, S. Trolier-McKinstry, and S. Kalinin, Proc. Natl. Acad. Sci. U. S. A. **107**(16), 7219 (2010).
[37]K. Jayabal, A. Menzel, A. Arockiarajan, and S. M. Srinivasan, Comput. Mech. **48**(4), 421 (2011).
[38]K. Jayabal and A. Menzel, Comput. Mater. Sci. **64**, 66 (2012).